Technical Progress Report

First Quarter

(October 1, 1992 to December 31, 1992)

DOE/PC/92246--T1

DE93 011460

DEVELOPMENT OF ENHANCED SULFUR REJECTION PROCESSES

by

R.-H. Yoon, G. Luttrell, G. Adel and P.E. Richardson
Center for Coal and Minerals Processing
Virginia Polytechnic Institute and State University
Blacksburg, Virginia 24021-0258

Contract No.: DE-AC22-92PC92246

Prepared for:

U.S. Department of Energy
Pittsburgh Energy Technology Center
P.O. Box 10940
Pittsburgh, PA 15236-0940

March 23, 1993

Contracting officer's representative: Richard Read

US/DOE Patent Clearance is not required prior to the publication of this document.

ABSTRACT

Research at Virginia Tech led to two complementary concepts for improving the removal of inorganic sulfur from much of the Eastern U.S. coals. One controls the surface properties of coal pyrite (FeS_2) by electrochemical potential control, referred to as the Electrochemically Enhanced Sulfur Rejection (EESR) Process. The second controls the flotation of middlings, i.e., particles composed of pyrite with coal inclusions by using polymeric reagents to react with pyrite and convert the middlings to hydrophilic particles, and is termed the Polymer Enhanced Sulfur Rejection (PESR) Process. These new concepts are based on recent research establishing the two main reasons why flotation fails to remove more than about 50% of the pyritic sulfur from coal: superficial oxidization of liberated pyrite to form polysulfide oxidation products so that a part of the liberated pyrite floats with the coal; and hydrophobic coal inclusions in the middlings dominating their flotation so that the middlings also float with the coal. These new pyritic-sulfur rejection processes do not require significant modifications of existing coal preparation facilities, enhancing their adoptability by the coal industry. It is believed that they can be used simultaneously to achieve both free pyrite and locked pyrite rejection.

The technical research was initiated on October 1, 1992. During this reporting period, a detailed work plan and work schedule (Task 1) was developed and research has been initiated. For Task 2, samples of pyrite from Illinois No. 6 and Pittsburgh No. 8 coals were obtained and are being characterized. For Task 3, electrochemical studies were initiated on oxygen reduction and pyrite oxidation. These studies show that the mechanism of oxygen reduction on coal and mineral pyrite depends on pH and that the mechanism on Pittsburgh No. 8 coal pyrite is different than on mineral pyrite and on well-crystallized coal pyrite from China. For Task 5, microflotation of pyrite in a novel electrochemical cell was initiated. Recovery vs. potential curves for coal and mineral pyrite have been obtained.

TABLE OF CONTENTS

ABSTRACT i

TABLE OF CONTENTS ii

LIST OF FIGURES iii

INTRODUCTION 1

OBJECTIVES OF WORK, REPORTING PERIOD 1 2

RESULTS AND DISCUSSION 3

Task 1 - Project Planning 3

Task 2 - Characterization 3
2.1 Coal Samples and Characterization 3
2.2 SEM-IPS Analysis of Feed Samples 3
2.3 SEM-IPS Analysis of Flotation Products 3

Task 3 - Electrochemical Studies 4
3.1 Linear Voltammetric Sweeps 4
3.2 Determination of Reducing Potentials 16
3.3 Mechanisms/Kinetics of Pyrite Oxidation by Cyclic Voltammetry 16

Task 4 - In-Situ Monitoring of Reagent Adsorption on Pyrite 26
4.1 Mechanistic Studies of Reagent Adsorption on Pyrite 26
4.2 Contact Angle Measurements of Reagents on Pyrite Surfaces 26

Task 5 - Bench Scale Testing of the EESR Process 27
5.1 Microflotation Tests 27
5.2 Galvanic Control Using Metal and Alloy Powders 31
5.3 Galvanic Control Using Sacrificial Anodes 31

Task 6 - Bench Scale Testing of the PESR Process 31

Task 7 - Modelling and Simulation 31

CONCLUSIONS 32

BIBLIOGRAPHY 33

LIST OF FIGURES

Figure 1: Ring-disc voltammograms for oxygen reduction on Chinese coal pyrite at pH 9.2 (ring at +0.24 V, the number specified is the electrode rotation speed in rpm)

Figure 2: Limiting current vs. electrode rotating speed for oxygen reduction on Chinese coal pyrite at pH 9.2

Figure 3: Disc voltammograms for oxygen reduction on Pittsburgh No. 8 coal pyrite (top) and mineral pyrite (bottom) at pH 9.2 (ring at +0.24 V, the number specified is the electrode rotation speed in rpm)

Figure 4: Ring-disc voltammograms for oxygen reduction on Chinese coal pyrite at pH 4.6 (ring at +0.54 V, dashed line is the current in nitrogen sparged solution and the number specified is the electrode rotation speed in rpm)

Figure 5: Ring-disc voltammograms for oxygen reduction on mineral pyrite at pH 4.6 (ring at +0.54 V, the number specified is the electrode rotation speed in rpm)

Figure 6: Ring-disc voltammograms for oxygen reduction on Pittsburgh No. 8 coal pyrite at pH 4.6 (ring at +0.54 V, the number specified is the electrode rotation speed in rpm)

Figure 7: Disc voltammograms for oxygen reduction at pH 6.8 for different pyrite samples (the number specified is the electrode rotation speed in rpm; top, Pittsburgh No. 8 coal pyrite; middle, Chinese coal pyrite; bottom, mineral pyrite)

Figure 8: Ring-disc voltammograms of different cycles with Chinese coal pyrite at pH 9.2 (ring at +0.24 V)

Figure 9: Ring-disc voltammograms of mineral pyrite at pH 9.2 with varying upper potential limit (ring at +0.24 V)

Figure 10: Comparison of ring-disc voltammograms of different pyrite specimens at pH 9.2 with ring potential being at +0.24 V

Figure 11: Ring-disc voltammograms of different pyrite samples at pH 4.6 with ring being held at +0.24 V

Figure 12: Ring-disc voltammograms of different pyrite samples at pH 6.8 with ring being held at +0.24 V

Figure 13: Illustration of the electrochemical-microflotation cell

Figure 14: Effect of potential on flotation recovery of mineral pyrite at different pH values (particle size 850-1190 μm)

INTRODUCTION

Recent work at the Center for Coal and Minerals Processing has identified two major reasons why even the most advanced coal cleaning technologies (without fine grinding) fail to meet what is normally a standard flotation separation for most mineral systems, i.e., a 90-95% rejection of pyrite from coal. They are:

i) ***superficial oxidation*** of pyrite as an inadvertent corrosion-type process that occurs during mining and processing, and

2) ***incomplete liberation*** of pyrite from coal such that a large fraction of the pyrite remains associated or locked with the coal as middlings.

The ***superficial*** oxidation produces a surface layer on liberated pyrite that is composed of excess sulfur (or polysulfides), which is inherently hydrophobic. Thus, even the fully-liberated pyrite can show a flotation response similar to that of coal when it is superficially oxidized, making the separation difficult. The ***incomplete*** liberation of pyrite from coal creates coal/pyrite composites which behave more like coal during flotation. Even tiny inclusions of coal in pyrite particles can render the composites floatable.

Research at Virginia Tech's Center for Coal and Mineral Processing (CCMP) suggests two solutions to these problems. These are ***Electrochemically-Enhanced Sulfur Rejection*** (EESR) and ***Polymer-Enhanced Sulfur Rejection*** (PESR) processes. The EESR concept represents a novel technique that prevents superficial oxidation of pyrite without using traditional

reducing reagents. It is based on using sacrificial anodes to prevent the oxidation of pyrite and, hence, its flotation. This technique is flexible enough to be implemented during the process of grinding, conditioning or flotation. The PESR process is based on synthesizing polymeric organic reagents whose functional groups react with pyrite, possibly via an electrochemical mechanism, while the hydrophilic polymer chains are stretched over the coal inclusions so that the pyrite-coal composite particles will not float. The EESR and PESR processes are complementary since the former suppresses the flotation of free pyrite while the latter suppresses middlings.

The overall objective of this research is to develop these processes into technologies for improving the rejection of pyritic sulfur from Eastern U.S. coals. If successful, a high degree of pyritic sulfur rejection could be achieved without having to micronize coal.

OBJECTIVES OF WORK, REPORTING PERIOD I

The objectives of this first reporting period were to develop and implement a detailed work plan covering the period of this project (September 30, 1992 to March 31, 1994). The work plan during this report period include the following tasks: i) electrochemical studies to determine the kinetics of oxygen reduction on pyrite, ii) mechanisms and kinetics of pyrite oxidation by cyclic voltammetry; and iii) microflotation tests to study the effect of controlling the electrochemical potential on flotation. All of these tasks were carried out according to the work plan. For this report, the terms coal pyrite and mineral pyrite, refer to pyrite derived from coal and from non-coal sources, respectively.

RESULTS AND DISCUSSION

Task 1 - Project Planning

A detailed work plan for the project was forwarded to DOE on January 12, 1993, and approved shortly thereafter. The plan includes a description of the research approach, seven detailed tasks to meet the overall project objectives, and a work schedule.

Task 2 - Characterization

Subtask 2.1: Coal Samples and Characterization

Run-of-mine coal samples of the Pittsburgh No. 8 and Illinois No. 6 seams were received in 55-gallon drums. The Pittsburgh No. 8 sample was pulverized and sized to 90-95% passing 28, 100 and 400 mesh, using a Raymond laboratory hammer mill. The samples are currently being analyzed to determine the moisture, ash, volatile matter, fixed carbon, total sulfur, pyritic sulfur, organic sulfur, and calorific value. Characterization of the Illinois No. 6 sample will be conducted during the next reporting period. Arrangements are being made to obtain run-of-mine Upper Freeport seam coal.

Subtask 2.2: SEM-IPS Analysis of Feed Samples

No work was scheduled during this reporting period.

Subtask 2.3: SEM-IPS Analysis of Flotation Products

No work was scheduled during this reporting period.

Task 3 - Electrochemical studies

Subtask 3.1: Linear Voltammetric Sweeps

Sulfides, including pyrite, undergo mixed potential, corrosion type reactions when they are exposed to oxygen and water. The anodic process represents sulfide dissolution in acid circuits and oxide/hydroxide formation in alkaline circuits. The cathodic process is generally the reduction of oxygen and has not been studied nearly as much as the anodic process. Oxygen reduction is important because in many cases it can control the rate of oxidation of pyrite.

The specific objective of the project during this report period was to determine the mechanisms and kinetics of oxygen reduction on coal and mineral pyrite. For this purpose, a rotating ring-disc electrode was used to provide a well-defined hydrodynamic system, in which the mass transfer of reactants to and from an electrode can be controlled and analytically calculated by solving the steady state diffusion equations. The maximum or limiting current (I_L) to a rotating disc electrode is given by the Levich equation (see e.g. Electrochemical Methods, Fundamentals and Applications, by Allen S. Bard and Larry R. Faulkner, John Wiley and Sons, Inc, 1980, p. 288):

$$I_L = 0.62nFD^{2/3}\nu^{-1/6}C_b\omega^{1/2} \qquad (1)$$

where n is the number of electrons in the rate determining step, D is the diffusion constant for the relevant species undergoing oxidation or reduction, ν is the kinematic viscosity, C_b is the concentration of the electro-active species in the bulk solution, and ω is the rotation rate of the electrode. This equation essentially represents how the stagnant boundary layer at the surface of a rotating electrode thins with increasing rotation rate. I_L corresponds to the current when

all of the species reaching the surface are reduced.

The ring electrode is concentric with the disc and separated from the disc by a small gap of nonconductive epoxy resin. Convective mass transfer in the rotating ring-disc system is such that soluble ions produced by an oxidation or reduction reaction at the disc convect parallel to the disc surface and the ring. By holding the ring at different potentials than the disc, the oxidation (or reduction) products formed at the disc can be reduced (or oxidized) at the ring. From the potentials at which the oxidation (or reduction) products are reduced (or oxidized), it is possible to identify the products.

The disc electrodes were made using both coal and mineral pyrite. The ring electrode was constructed from gold and the assembly was mounted using a nonconducting epoxy. A Pine RDE-4 double potentiostat was used to apply different potentials and a Pine rotating ring-disc assembly to rotate the electrodes. The pyrite disc electrodes were prepared using diamond core drills and contacted with a copper electrical lead. The electrode surfaces were abraded and polished using successively finer grades of silicon carbide paper from 240 to 600 grit. The samples were cleaned with acetone, hydrochloric acid and distilled water before each experiment.

Large specimens of mineral pyrite, originating from Huanzala, Peru, were obtained through Ward's Scientific Co. The Pittsburgh No. 8 coal pyrite was originally a chunk of 2.5"×2.3"×2" pyrite found in the "run-of-mine" coal sample. It contains approximately 5% coal on the surface. For comparison, a coal pyrite from Sichuan, China was also used. These coal pyrite samples were shiny, contained no visible specks of coal and had the appearance of mineral pyrite.

The buffer solutions used in all tests were prepared using reagent grade chemicals with the following compositions:

pH 4.6: 0.5 M CH_3COOH and 0.5 M CH_3COONa

pH 6.8: 0.05 M KH_2PO_4 and 0.0224 M NaOH

pH 9.2: 0.05 M $Na_2B_4O_7$

All potentials were measured against the saturated calomel electrode (SCE) and are reported against the standard hydrogen electrode (SHE). All linear sweep voltammetry was conducted at 20 mv/sec.

Figure 1 (top) shows linear potential sweeps from 0.24 to -0.75 V (SCE) on the Chinese coal pyrite disc electrode at pH 9.2 for rotation speeds of 250 to 4000 rpm in a solution saturated with oxygen. At the beginning of the sweeps, the current is controlled by the electron transfer process (activation control) and is only slightly dependent on rotation rate (ω). As the potential becomes more negative, the diffusion of oxygen to the disc surface gradually predominates over the charge transfer process in determining the reaction rate and, hence, the current is increasingly dependent on rotation speed. The reaction rate is controlled by the mass-transfer process at potentials of about -0.75 V. The plot of I_L vs. $\omega^{1/2}$ is shown in Figure 2 to be linear as predicted by the Levich equation. Figure 1 (bottom) also shows the ring currents when the ring was held at 0.24 V. This potential is high enough to oxidize hydrogen peroxide (H_20_2) produced during the linear sweeps on the disc. The absence of a ring-current from 0.24 to -0.65 V suggests that the reduction of oxygen proceeds to water by the overall 4-electron process:

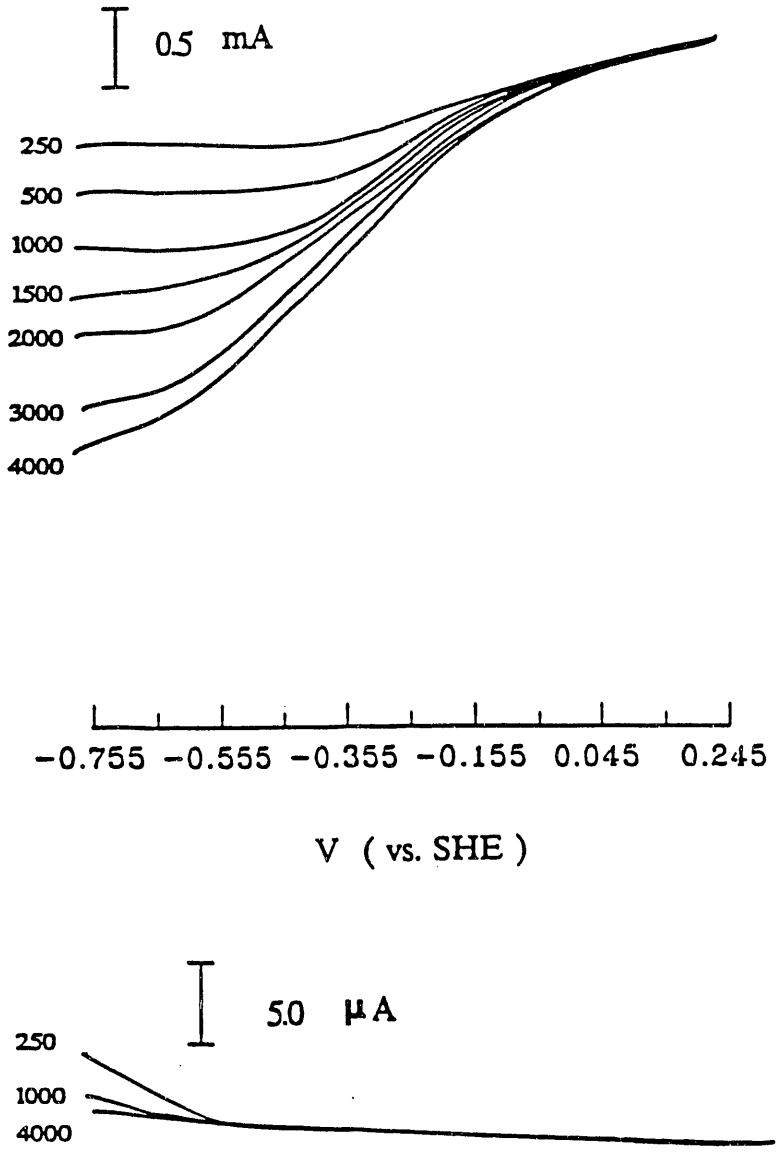

Figure 1. Ring-disc voltammograms for oxygen reduction on Chinese coal pyrite at pH 9.2 (ring at +0.24 V, the number specified is the electrode rotation speed in rpm)

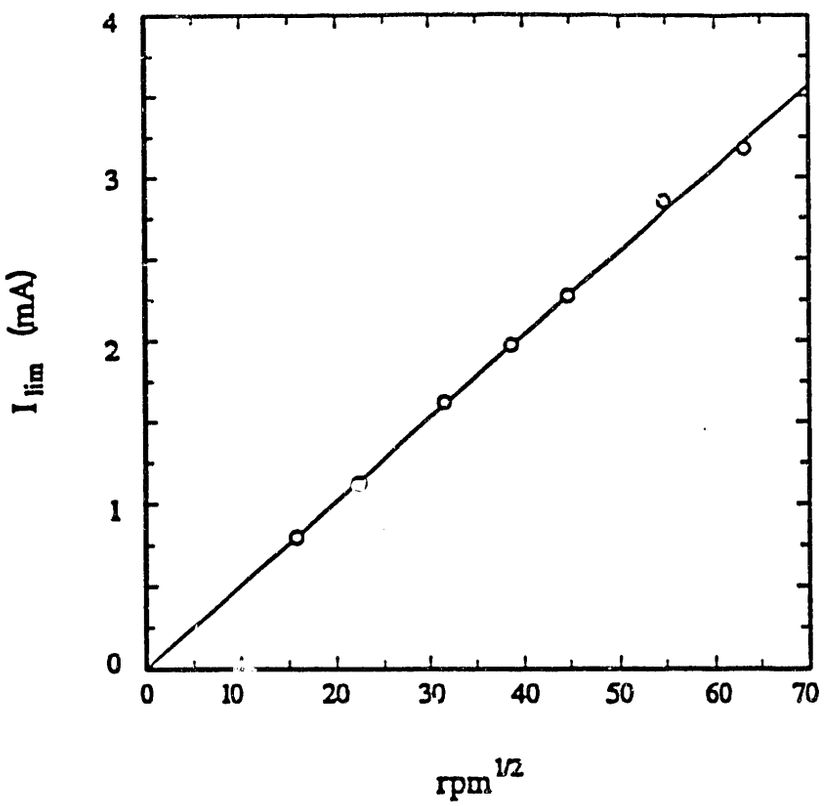

Figure 2. Limiting current vs. electrode rotating speed for oxygen reduction on Chinese coal pyrite at pH 9.2

$$O_2+2H_2O+4e^-=4OH^- \quad (2)$$

i.e., there is no intermediate soluble species generated during the oxygen reduction process at pH 9.2 (Biegler, Rand and Woods, 1975,1976; Ahmed, 1978). The small ring current observed at potentials < -0.65 V is due to the cathodic decomposition of pyrite and will be discussed later. The results obtained with Pittsburgh No. 8 coal and mineral pyrite are similar and the disc voltammograms are shown in Figure 3.

Oxygen reduction on pyrite proceeds via a different route from the above in acidic aqueous solutions. Figure 4 shows linear sweep voltammograms for the Chinese coal pyrite electrode at pH 4.6 from 0.24 to -0.75 V in a solution saturated with O_2. In the activation-controlled region, i.e., before the limiting currents are reached, there are two distinct cathodic reduction processes occurring, as evidenced by the change in slope of the curves at about -0.05 V. The ring, held at 0.54 V during the potential sweep on the disc, shows that an intermediate species is produced beginning at about -0.05 V. This is attributed to hydrogen peroxide produced on the disc by the reaction:

$$O_2+2H^++2e^-=H_2O_2 \quad (3)$$

followed by its re-oxidation on the ring. The ring current reaches a maximum at about -0.25 V. When the limiting current on the disc is reached (-0.35 to -0.55 V), the overpotential is sufficiently large that the intermediate hydrogen peroxide is also reduced at the disc to OH^- and less hydrogen peroxide diffuses to the ring. Consequently, the ring current resulting from re-oxidation of hydrogen peroxide drops. At more negative potentials, cathodic decomposition of pyrite again occurs, and a distinct ring current is produced by a soluble product of pyrite

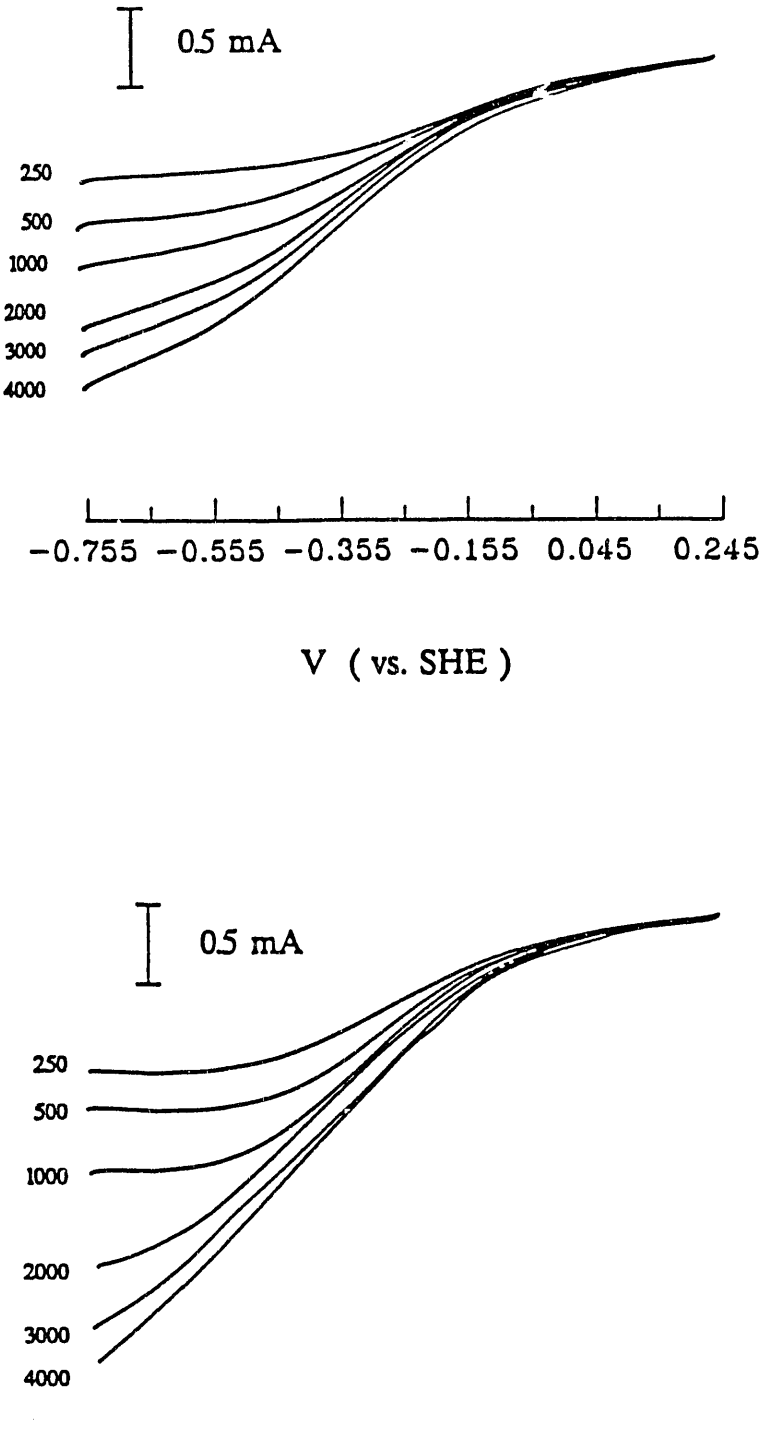

Figure 3. Disc voltammograms for oxygen reduction on Pittsburgh No.8 coal pyrite (top) and mineral pyrite (bottom) at pH 9.2 (ring at +0.24 V, the number specified is the electrode rotation speed in rpm)

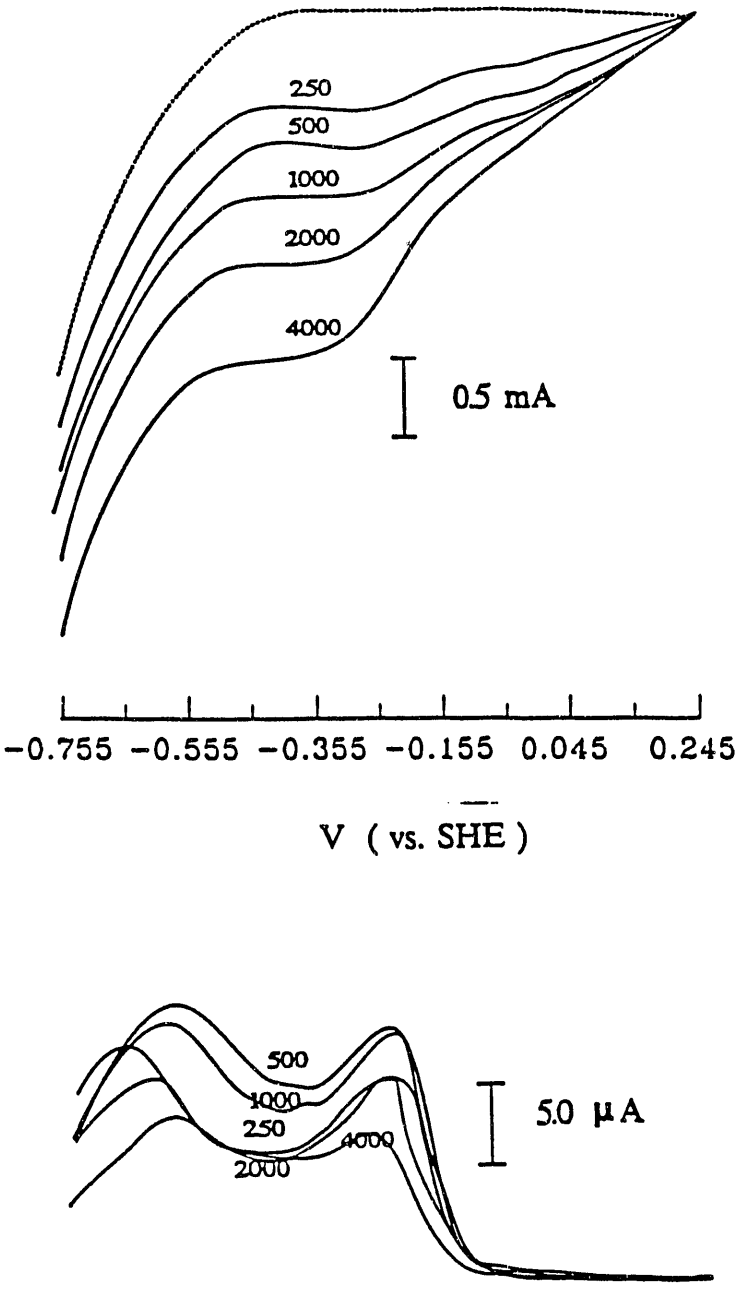

Figure 4. Ring-disc voltammograms for oxygen reduction on Chinese coal pyrite at pH 4.6 (ring at +0.54 V, dashed line is the current in nitrogen sparged solution and the number specified is the electrode rotation speed in rpm)

decomposition. That the ring current due to decomposition of mineral pyrite is smaller than that of coal pyrite may suggest that the latter is oxidized faster.

The data for mineral pyrite (Figure 5) are similar to those for the Chinese coal pyrite; however, Pittsburgh No. 8 coal pyrite exhibited different behavior at pH 4.6. For Pittsburgh No. 8 coal pyrite, the voltammetry curve on the disc electrode (Figure 6) does not show a change in the slope prior to the diffusion-limited current. Correspondingly, there is no ring current peak at -0.25 V, as observed with the two other samples of pyrite. This indicates that oxygen can be reduced all the way to water on Pittsburgh No. 8 coal pyrite, with a negligible amount of hydrogen peroxide being formed as an intermediate.

The behavior of oxygen reduction on pyrite at pH 6.8 is similar to that at pH 9.2 for all three pyrite samples studied; there was no distinct changes in the slope of current vs. potential curves for disc electrodes observed and no hydrogen peroxide was detected on the ring electrode. The voltammograms for the disc electrodes of three pyrite specimens are shown together in Figure 7. The rate of oxygen reduction on the Chinese coal pyrite and the mineral pyrite are similar; the rate on Pittsburgh No. 8 coal pyrite is quite different.

Figure 7 shows that on mineral pyrite, oxygen reduction at pH 6.8 shows a higher current and the mass-transfer limited current is acquired at lower potentials than for the Pittsburgh No. 8 coal pyrite. For Chinese coal pyrite, although the current is higher at pH 6.8 than at pH 9.2, the potential at which the diffusion-limited current is reached does not change remarkably as the solution pH changes from 9.2 to 6.8. For the Pittsburgh No. 8 coal pyrite, the oxygen reduction current increases considerably with decreasing pH from 9.2 to 6.8, and the

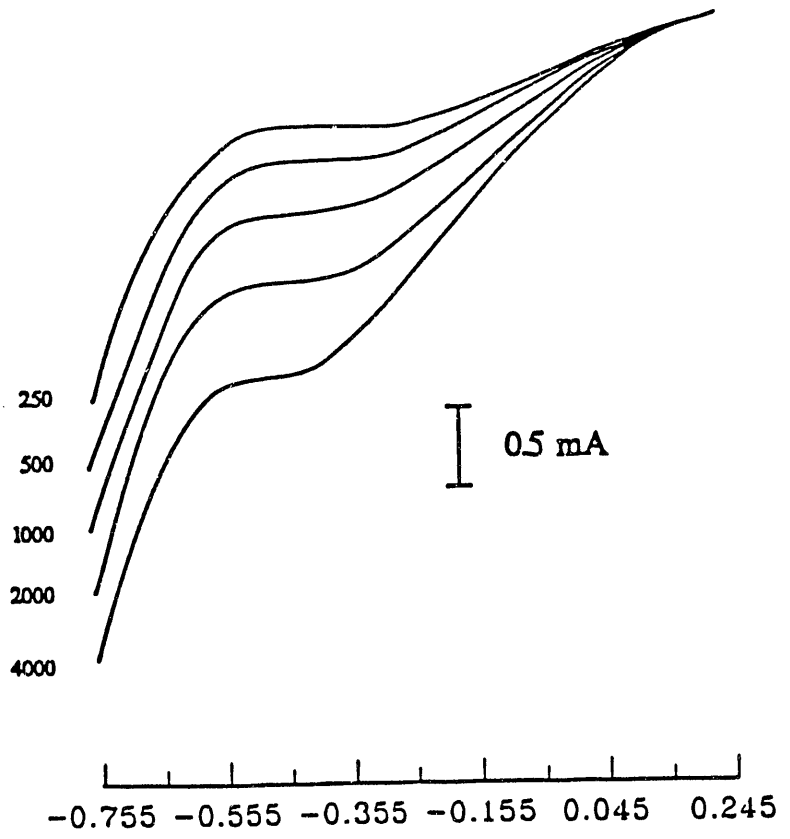

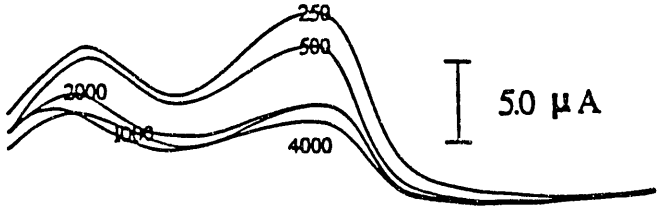

Figure 5. Ring-disc voltammograms for oxygen reduction on mineral pyrite at pH 4.6 (ring at +0.54 V, the number specified is the electrode rotation speed in rpm)

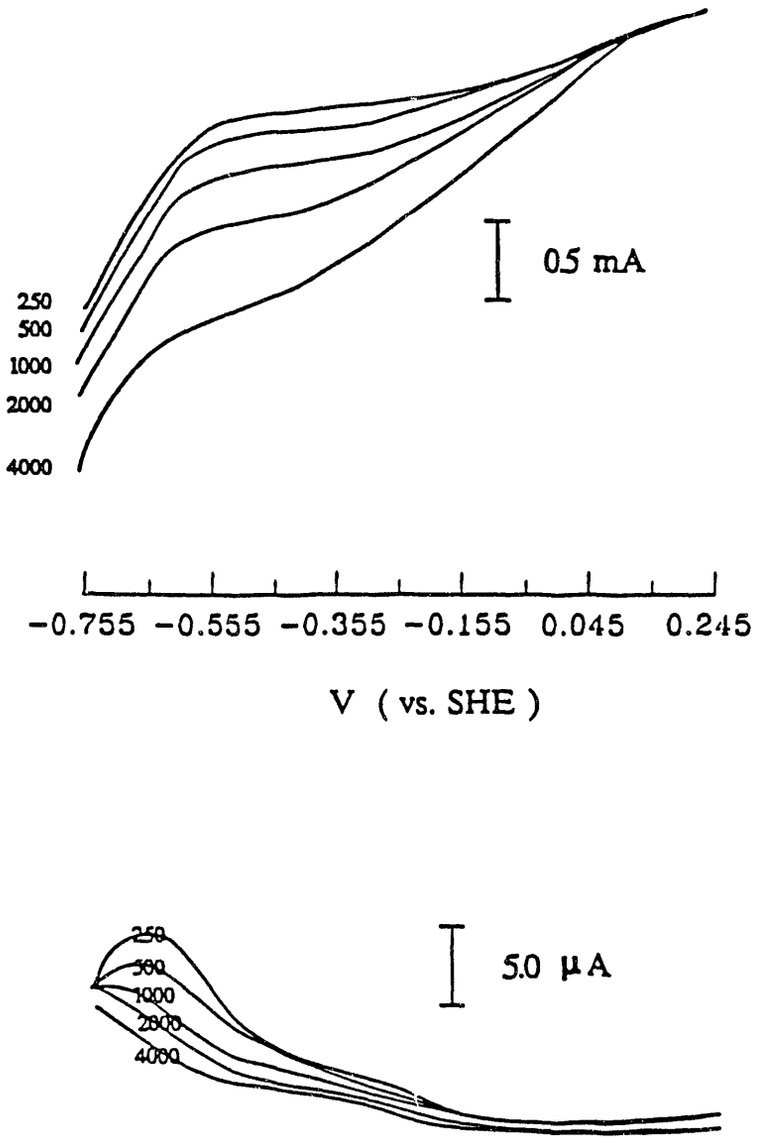

Figure 6. Ring-disc voltammograms for oxygen reduction on Pittsburgh No. 8 coal pyrite at 4.6 (ring at +0.54 V, the number specified is the electrode rotation speed in rpm)

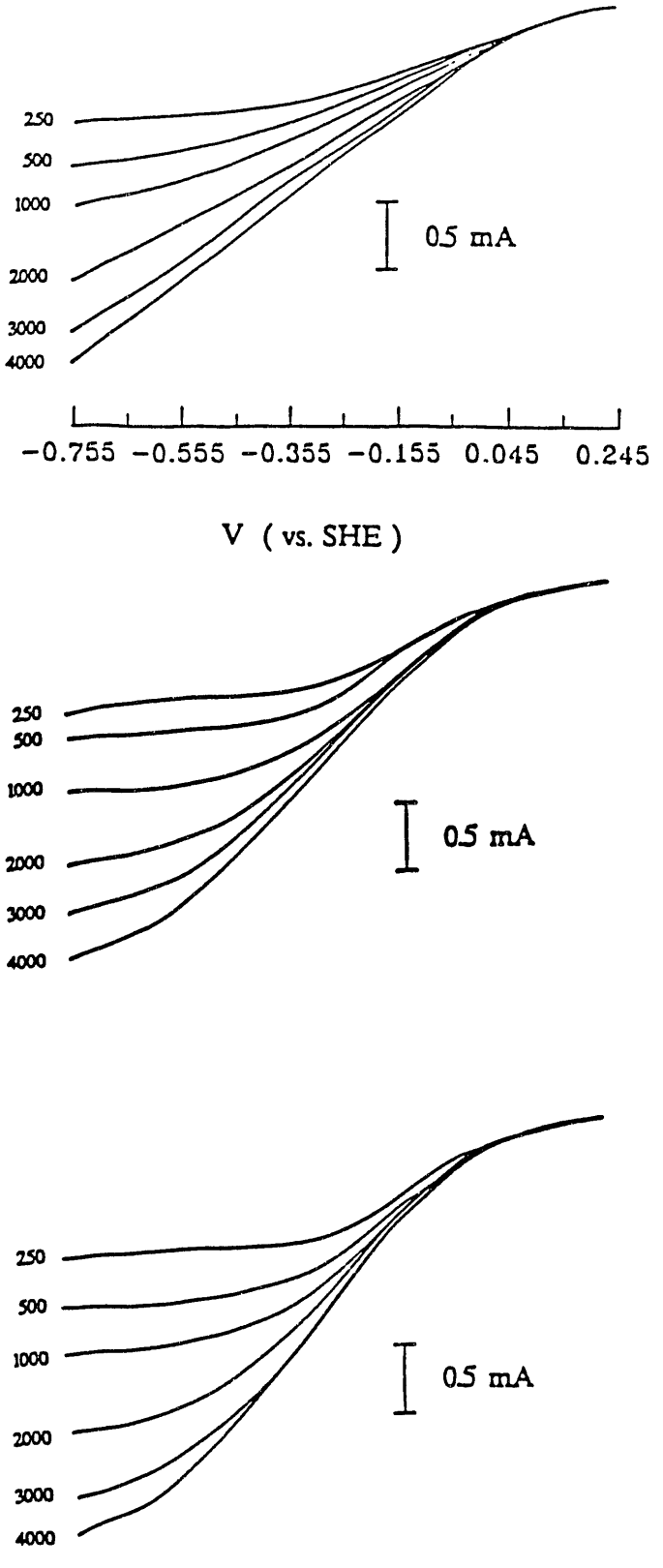

Figure 7. Disc voltammograms for oxygen reduction at pH 6.8 for different pyrite samples (the number specified is the electrode rotation speed in rpm; top, Pittsburgh No. 8 coal pyrite; middle, Chinese coal pyrite; bottom, mineral pyrite)

potential where the diffusion-limited current is reached shifts significantly, especially at the higher electrode rotation speed. All three pyrite samples examined show a consistent characteristic: the magnitude of the diffusion-limited current for oxygen reduction follows the order: pH 6.8 > pH 9.2 > pH 4.6. The low oxygen reduction rate at pH 4.6 may be attributed to the decomposition of pyrite. On the other hand, that the oxygen reduction rate is lower at pH 9.2 than pH 6.8 may be attributed to the formation of iron hydroxide and iron polysulfide.

Subtask 3.2: Determination of Reducing Potentials

No work was scheduled during this reporting period.

Subtask 3.3: Mechanism/Kinetics of Pyrite Oxidation by Cyclic Voltammetry

The objective of the research during this report period was to study the mechanism and kinetics of pyrite oxidation, and in particular to determine if the ring-disk technique could be used to detect soluble oxidation or reduction products being produced on pyrite. It has been established (Hamilton and Woods, 1981) that at potentials anodic of the rest potential, pyrite undergoes anodic oxidation/dissolution reactions through several different pathways, as suggested by the following reactions (Young et al., 1988; Trahar, 1984; Buckley et al., 1985):

$$FeS_2 = Fe_{1-x}S_2 + xFe^{2+} + 2xe^- \quad (4)$$

$$FeS_2 + 3H_2O = Fe(OH)_3 + 2S^o + 3H^+ + 3e^- \quad (5)$$

$$FeS_2 + 3xH_2O = xFe(OH)_3 + Fe_{1-x}S_2 + 3xH^+ + 3xe^- \quad (6)$$

$$nFeS_2=(n-2)Fe^{2+}+2FeS_n+2(n-2)e^- \quad (7)$$

$$FeS_2+11H_2O=Fe(OH)_3+2SO_4^{2-}+19H^++15e^- \quad (8)$$

$$FeS_2+6H_2O=Fe(OH)_3+S_2O_3^{2-}+9H^++7e^- \quad (9)$$

The reactions (5-9) have been written for basic solutions assuming ferric hydroxide is the stable oxidation product. Soluble ferric and ferrous hydroxide complexes may also be formed. Reactions 4-7 are generally considered to be responsible for the flotation of pyrite under mildly oxidizing conditions. The hydrophobic species may be elemental sulfur or polysulfides FeS_n.

Figure 8 shows five consecutive voltammetry curves on Chinese coal pyrite in nitrogen sparged solution at pH 9.2. The materials and experimental conditions used for these studies were the same as for Subtask 3.1 discussed above. The anodic peak at -0.04 V has been attributed to the oxidation of $Fe(OH)_2$ to $Fe(OH)_3$; the cathodic peak at -0.35 V to the reduction of the $Fe(OH)_3$ to $Fe(OH)_2$. Figure 8 (bottom) shows the ring current observed with the ring held at 0.24 V during the potential sweep on the disc from 0.4 to -0.75 back to 0.4 V. A ring current is observable at -0.05 V. The species responsible for the ring current has not yet been identified but it is believed to be oxidation of HS^-. At the most negative potentials a further increase in ring current is observed, which can be attributed to oxidation at the ring of the reduction product generated at the disc at potentials < -0.65 V. The most likely disc reaction is (Zhu et al., 1991):

$$FeS_2+2H_2O+4e^-=Fe+2HS^-+2OH^- \quad (10)$$

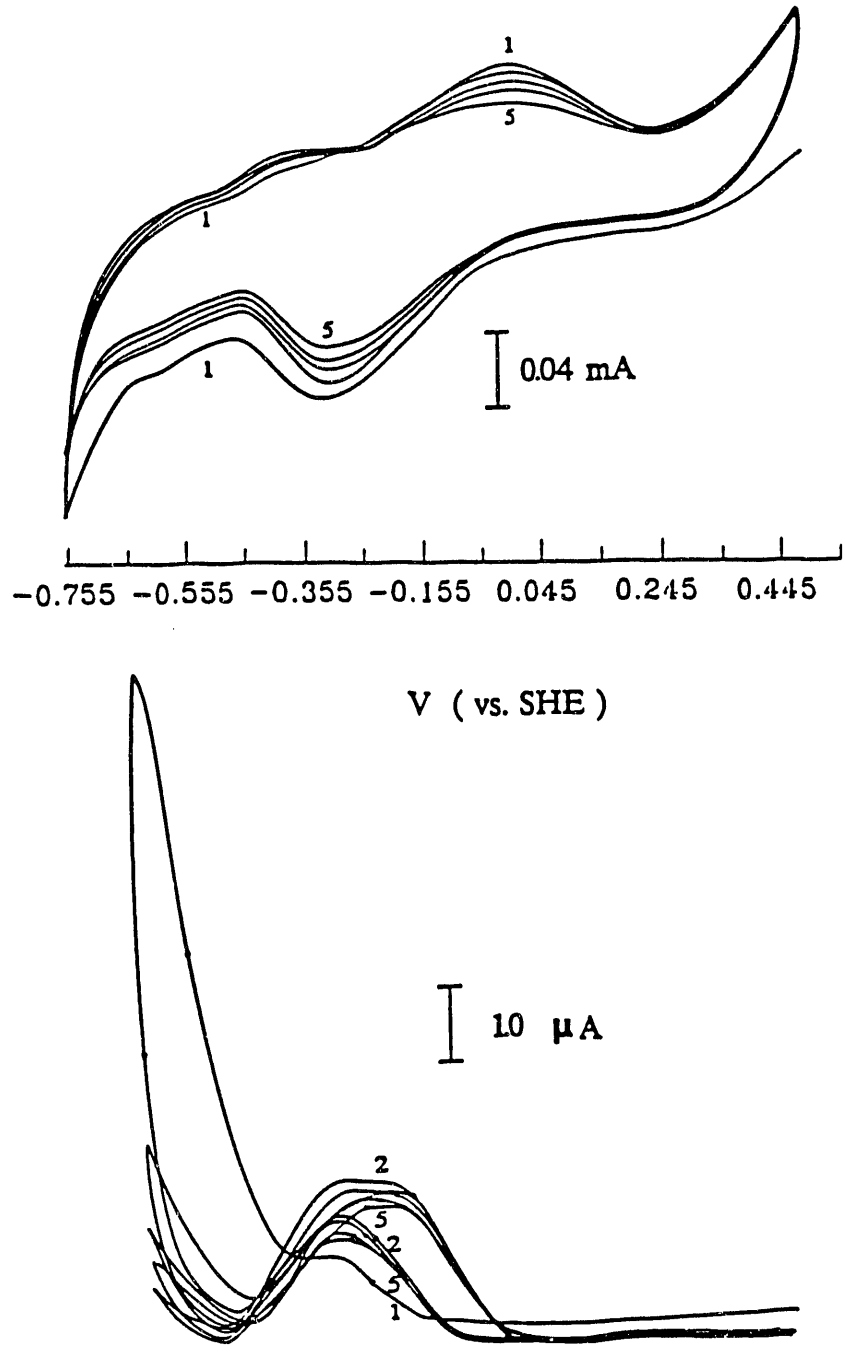

Figure 8. Ring-disc voltammograms of subsequent cycles with Chinese coal pyrite at pH 9.2 (ring at +0.24 V)

Interestingly, on the subsequent anodic sweep, an additional oxidation current is observed on the ring, implying that there is a soluble oxidation species produced at the disc on the initial portion of the positive going sweep, and that this oxidation product can be further oxidized at the ring. This has not been reported before. It is believed that the reactions involve either soluble iron-hydroxide complexes:

$$Disc:\ Fe + OH^- = Fe(OH)^+_{soluble} + 2e^- \quad (11)$$

$$Ring:\ Fe(OH)^+ + 2OH^- = Fe(OH)_3^+ + e^-, \quad (12)$$

or the reduction/oxidation of polysulfides.

Figure 9 shows the effect of the upper potential limit on the voltammetry curve of mineral pyrite at pH 9.2. It is interesting that the variation of the limit from 0.24 V, where transpassive oxidation of pyrite is negligible, to +0.54 V, where significant transpassive oxidation takes place, does not cause a corresponding increase in the cathodic peak at -0.35 V. This indicates that the oxidation of pyrite at high positive potentials does not produce significant amounts of insoluble ferric hydroxide, as suggested by Equations 5 and 6. One explanation is that hydrogen ions, produced during the oxidation of pyrite at high potentials, reduce the local pH of the solution in the vicinity of the electrode and dissolves some of the ferric hydroxide.

Mineral and Pittsburgh No. 8 coal pyrite exhibit voltammetry curves similar to those for Chinese coal pyrite. Figure 10 shows the second-cycle disc voltammogram and ring current at pH 9.2 for comparison. It is quite obvious that both of the coal pyrites are more reactive than mineral pyrite.

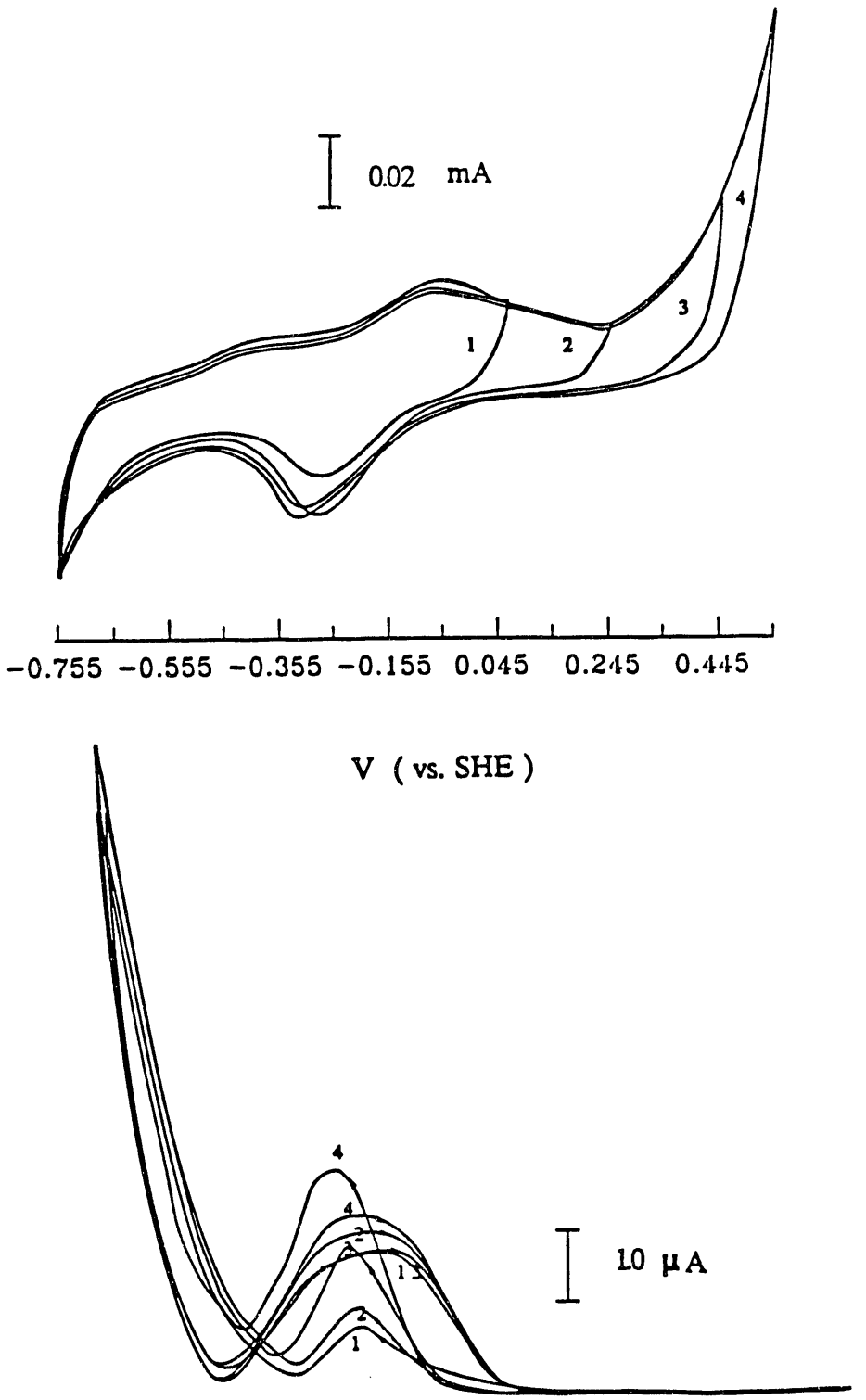

Figure 9. Ring-disc voltammograms of mineral pyrite at pH 9.2 with varying upper potential limit (ring at +0.24 V)

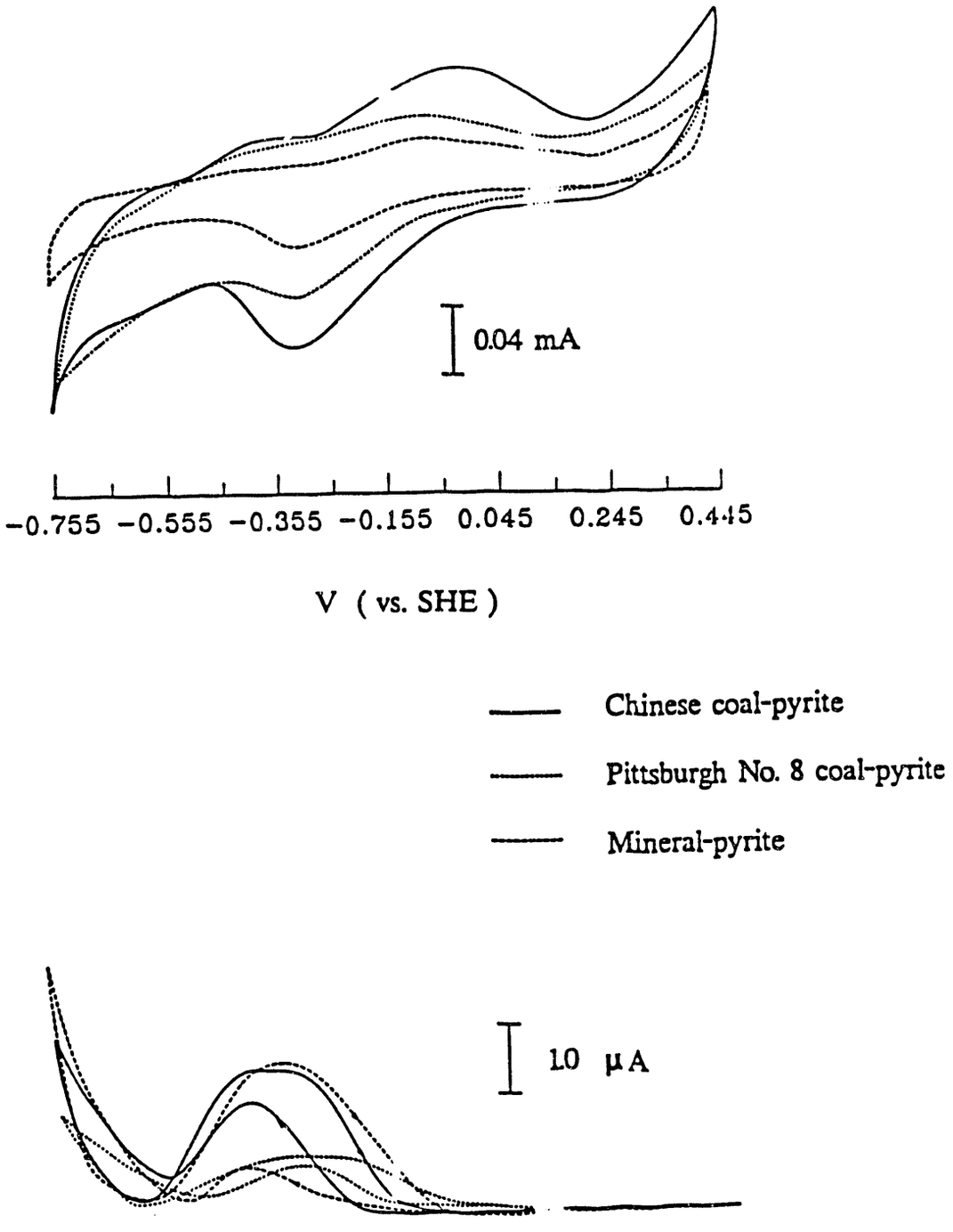

Figure 10. Comparison of ring-disc voltammograms of different pyrite specimens at pH 9.2 with ring potential being at +0.24 V

At acidic pH's, pyrite shows a significantly different electrochemical behavior than at pH 9.2. Figure 11 illustrates the voltammetry curves and ring currents between -0.4 V and +0.55 V at pH 4.6 when the potential of the ring electrode was held at 0.24 V. The lower limit of potential was determined based on the observation that potentials more negative than -0.4 V cause high currents, indicating excessive decomposition of pyrite and significant hydrogen evolution. The upper limit was chosen to avoid the unnecessary oxidation of pyrite. It can be seen that the cathodic peak at -0.18 V on mineral and Chinese coal pyrite (-0.3 V on Pittsburgh No. 8 coal pyrite) gives rise to the peak on the ring electrode. The probable reactions are:

$$Disc: \ Fe(OH)_3 + H^+ + e^- = Fe(OH)_2 + H_2O \qquad (13)$$

$$Ring: \ Fe(OH)_2 + H_2O = Fe(OH)_3 + H^+ + e^- \qquad (14)$$

The small cathodic current peak at -0.05 V for mineral and Chinese coal pyrite (0 V for Pittsburgh No. 8 coal pyrite) may be due to the reaction (Hamilton and Woods, 1981):

$$Fe(OH)_3 + S + 3e^- = FeS + 3OH^- \qquad (15)$$

Unlike at pH 9.2, no ring current was observed during the initial portion of the anodic potential sweep on the disc electrode at pH 4.6. The anodic peak was observed at -0.08 V for all three pyrite specimens and may represent the oxidation of $Fe(OH)_2$ produced during the former cathodic sweep:

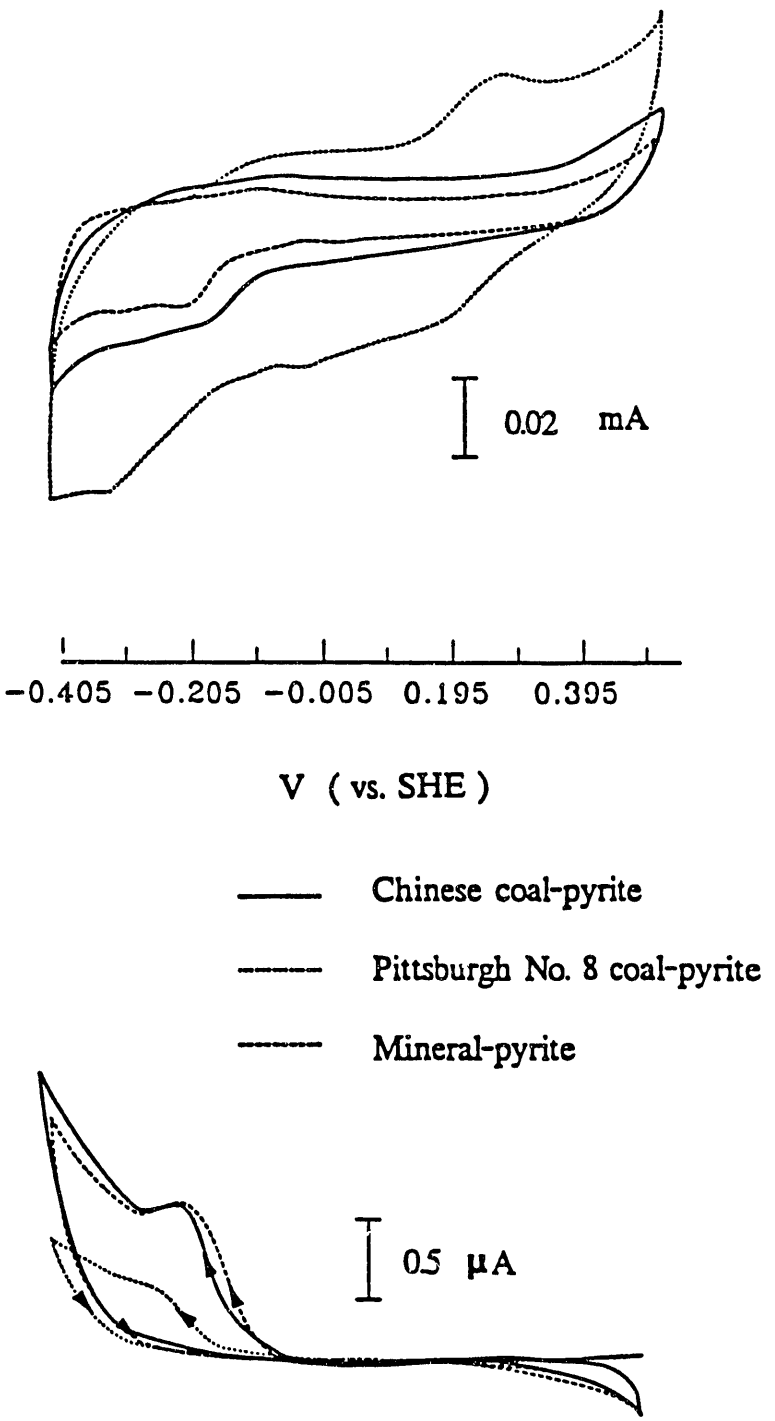

Figure 11. Ring-disc voltammograms of different pyrite samples at pH 4.6 with ring being held at +0.24 V

$$Fe(OH)_2 + OH^- = Fe(OH)_3 + e^- \quad (16)$$

Only Pittsburgh No. 8 coal pyrite exhibits an additional anodic current at +0.3 V which is attributed to the anodic oxidation reaction (Hamilton and Woods, 1981; Ahlberg et al., 1990):

$$FeS_2 = Fe^{2+} + 2S + 2e^- \quad (17)$$

or to the reactions expressed in Equations 4 to 7.

Comparison of the currents in Figure 11 clearly indicate that Pittsburgh No. 8 coal pyrite is the most active and mineral pyrite the least active while the Chinese coal pyrite is in-between. However, mineral pyrite generates more soluble products by the cathodic reduction reaction than Chinese coal pyrite while Pittsburgh No. 8 coal pyrite produces the least.

Figure 12 shows the ring-disc electrode voltammograms for three pyrite specimens at pH 6.8. The ring electrode was held at 0.24 V. While mineral pyrite behaves similarly to Chinese coal pyrite, Pittsburgh No. 8 coal pyrite demonstrates considerably different characteristics. For mineral and Chinese coal pyrite, the cathodic current peak on the disc electrode is observed at -0.1 V and results in the ring current peak. The reactions can be represented as:

$$Disc: \; Fe(OH)_3 + e^- = Fe(OH)_2 + OH^- \quad (18)$$

$$Ring: \; Fe(OH)_2 + OH^- = Fe(OH)_3 + e^- \quad (19)$$

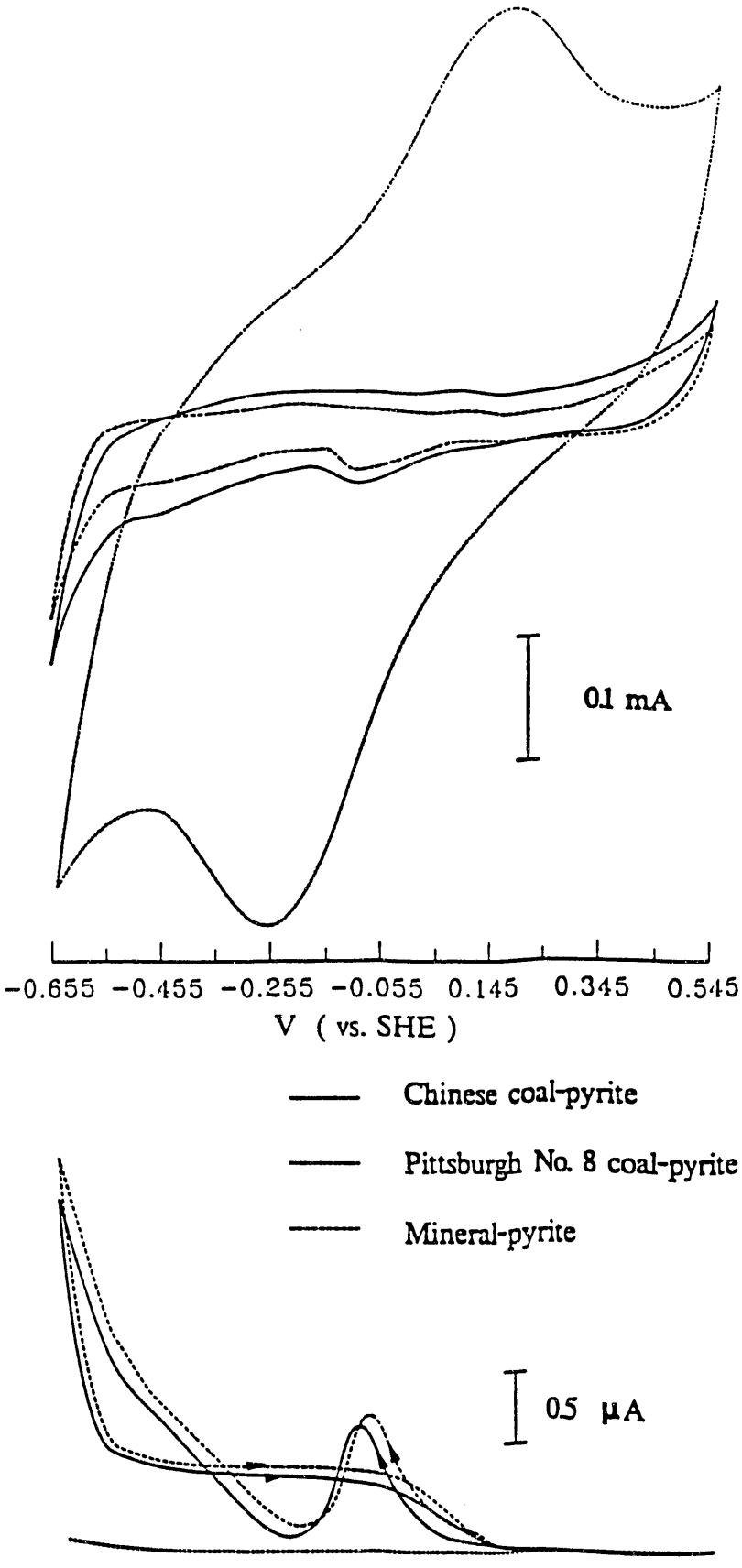

Figure 12. Ring-disc voltammograms of different pyrite samples at pH 6.8 with ring being held at +0.24 V

Pittsburgh No. 8 coal pyrite, however, exhibits a cathodic current peak at -0.25 V which does not yield a corresponding ring current peak, implying that no soluble species is formed during the cathodic reaction. This current peak may be attributed to the reduction of ferric hydroxide to iron without ferrous species being the intermediate due to the high reactivity of this pyrite:

$$Fe(OH)_3+3e^-=Fe+3OH^- \quad (20)$$

The anodic peak at -0.15 V is believed to be the reverse of this reaction.

The anodic wave at approximately 0.05 V is possibly due to either of the reactions (Zhu et al., 1991, 1992):

$$FeS_2+xH_2O=FeOH^{2+}+S_2O_x^{2-}+(2x-1)H^++(2x-1)e^- \quad (21)$$

$$Fe(OH)_2+OH^-=Fe(OH)_3+e^- \quad (22)$$

Task 4 - In Situ Monitoring of Reagent Adsorption on Pyrite

No work was scheduled during this reporting period.

Subtask 4.1 Mechanistic Studies of Reagent Adsorption on Pyrite

No work was scheduled during this reporting period.

Subtask 4.2 Contact Angle Measurements of Reagents on Pyrite Surfaces

No work was scheduled during this reporting period.

Task 5 - Bench-Scale Testing of the EESR Process

Subtask 5.1 Microflotation Tests

The objective of the research this reporting period was to use an electrochemical-microflotation cell to directly determine the dependence of the flotation of pyrite on electrochemical potential. The advantage of this technique is that no chemical reagents interfere with the determination of the recovery-potential behavior.

Figure 13 illustrates the electrochemical-microflotation cell utilized for studies on particulate beds. A coiled platinum lead (F) is connected to the mineral bed to serve as the working electrode. It rests on a glass frit (E) and is in intimate contact with the mineral bed. The counter electrode is a platinum wire housed in a fine porosity fritted tube (H). The tube containing the counter electrode is used as a plunger to compact the particles to ensure good physical and electrical contact throughout the bed. The fine porosity frit (ASTM 4-5.5 μm) minimizes diffusion of solution species between the counter and working electrode compartments. Potentials are measured against a saturated Calomel electrode using a Luggin capillary connection through port B. Ports A and C respectively serve as the inlet and the outlet for electrolyte circulation. The total electrolyte volume in the cell, circulation tubing and pump is about 20 ml.

Flotation recovery is determined by raising the counter electrode plunger until the fritted tube is above the center tube but is still making electrical contact with the electrolyte, as illustrated by its position in Figure 13. Nitrogen gas entering through port D is bubbled through the frit and bed, and any particles levitated by the bubbles are deflected by the counter electrode

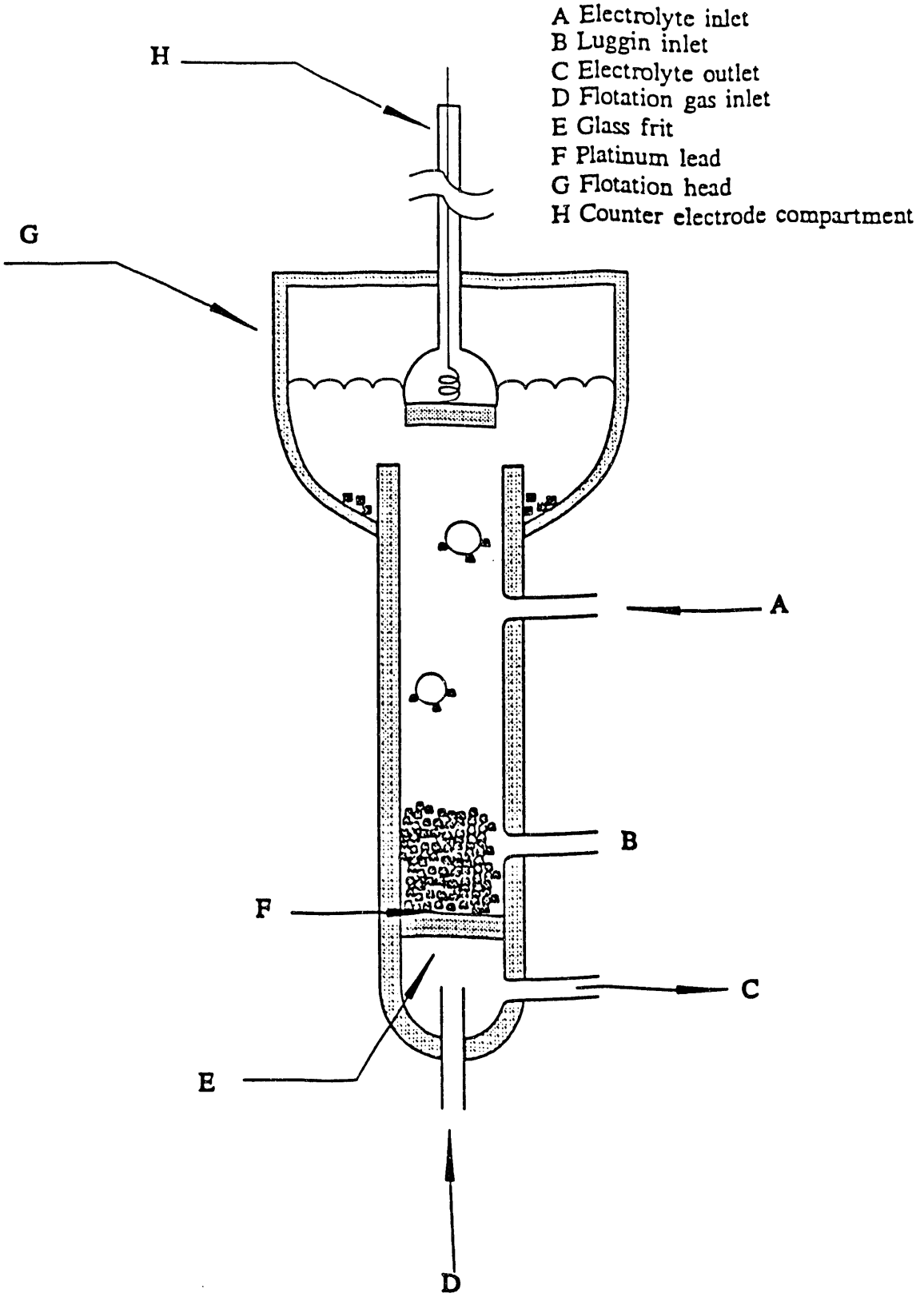

Figure 13. Illustration of the electrochemical-microflotation cell

compartment and deposited around the outside of the center tube. After flotation is complete, the cell head (G) can be raised to return the particles back to the bed.

The bed potential is controlled with a PAR 273 potentiostat and the current-voltage curves recorded on a Hewlett Packard 7015 B X-Y recorder. The electrolyte is continuously circulated through the cell at a rate of 25-30 ml/min. The pump element and flow tubing are Teflon to minimize extraneous contaminants. A 1.5 g sample of pyrite with an approximate area of 12 cm^2/g produces a mineral surface area to electrolyte volume ratio of 0.5 cm^{-1}.

Initial flotation tests were done with coarse particles in the 1190-850 μm (mesh sizes) size fraction. The samples and reagents were the same as those used in Task 3.1 above. As shown in Figure 14, no flotation of mineral pyrite was observed at neutral and alkaline pH over the entire potential region examined. As mentioned previously, elemental sulfur, metal-deficient sulfides or polysulfides are hydrophobic oxidation products capable of inducing flotation. The apparent lack of flotation of pyrite at any potential suggests that under neutral and alkaline conditions, most of the hydrophobic species formed on the surface may be covered by iron oxides/hydroxides. Under acidic conditions, the formation of iron oxides/hydroxides are not favored and most of the hydrophobic sites created from pyrite oxidation may render the coarse pyrite particles floatable. *An important conclusion drawn from Figure 14 is that pyrite can be depressed by controlling the potential under either reducing or oxidizing conditions.*

Interestingly, the above results could not be reproduced with coal pyrite. Coal pyrite did not exhibit flotation of particles of the 1190-850 μm size fraction even at pH 4.6. While the complete explanation for this difference is not yet available, one possible reason is that coal pyrite is more reactive than mineral pyrite and the partially oxidized hydrophobic sulfur

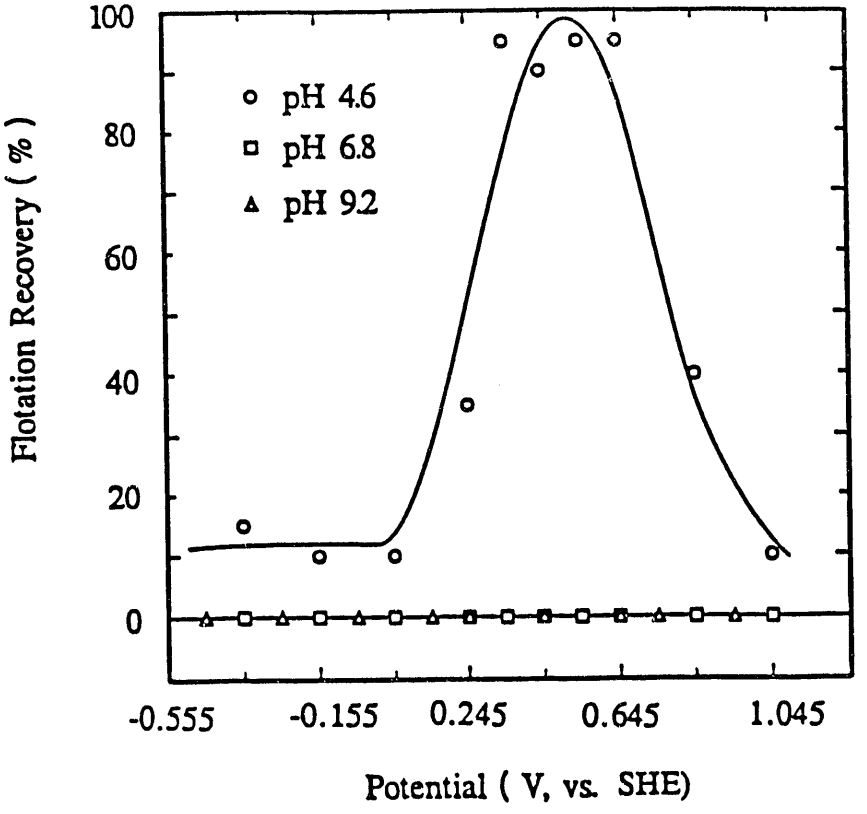

Figure 14. Effect of potential on flotation recovery of mineral pyrite at different pH values (particle size 850-1190 μm)

intermediates on the surface can be oxidized more readily to thiosulfate or sulfate, thereby removing hydrophobic sulfur. The removal of sulfur together with the increased presence of iron oxides/hydroxides may inhibit the flotation of large particles. This possibility will be verified using X-ray Photoelectron Spectroscopy (XPS) and the results will be provided in a future report. Preliminary experiments on coal pyrite particles 150 to 210 μm under different pH conditions demonstrated finite flotation over a wide range of pH, indicating that the coal pyrite does exhibit a certain degree of hydrophobicity upon superficial oxidation. Apparently, the electrochemical flotation cell used in the present work is not sensitive enough to detect the relatively low hydrophobicity created by superficial oxidation. Studies are continuing to better elucidate the difference in flotation behavior of coal and mineral pyrite.

Subtask 5.2 Galvanic Control Using Metal and Alloy Powders

No work was scheduled during this reporting period.

Subtask 5.3 Galvanic Control Using Sacrificial Anodes

No work was scheduled during this reporting period.

Task 6 - Bench-Scale Testing of the PESR Process

No work was scheduled during this reporting period.

Task 7 - Modelling and Simulation

No work was scheduled during this reporting period.

CONCLUSIONS

1. Using the ring-disc electrode technique, hydrogen peroxide has been detected as an intermediate oxygen reduction product on pyrite at pH 4.6, but not at pH 6.8 and pH 9.2.
2. Soluble iron hydroxide complexes or polysulfides are produced on all three pyrite samples at pH 4.6, 6.8 and 9.2 during cathodic reduction, but only at pH 9.2 during anodic oxidation.
3. Coal pyrite, particularly Pittsburgh No. 8, is more reactive than mineral pyrite with respect to both oxygen reduction and the oxidation of the mineral itself.
4. Strong collectorless (self-induced) flotation of coarse pyrite particles is observed for mineral pyrite at pH 4.6. This is in agreement with voltammetry studies; the likely reaction inducing the strong floatability of pyrite can be correlated with oxidation/reduction reactions on the voltammograms.
5. Pyrite floatability can be controlled by controlling the potential of pyrite bed-electrodes. Complete depression occurs under reducing and strongly oxidizing conditions.

BIBLIOGRAPHY

Ahlberg, E., Forssberg, K.S.E. and Wang X., 1990, "The surface oxidation of pyrite in alkaline solution", *J. of Appl. Electrochemistry*, **20**, 1033-1039.

Ahmed, S.M., 1978, "Electrochemical studies of sulphides, I. The electro-catalytic activity of galena, pyrite and cobalt sulphide for oxygen reduction in relation to xanthate adsorption and flotation", *Int. J. Min. Proc.*, **5**: 163-174.

Biegler, T., Rand, D.A.J., and Woods, R., 1975, "Oxygen reduction on sulphide minerals Part I. Kinetics and mechanisms at rotated pyrite electrodes", *J. Electroanal. Chem. Interfacial Electrochem.*, **60**: 151-162.

Biegler, T., Rand, D.A.J., and Woods, R., 1976, "Oxygen reduction on sulphide minerals Part II. Relations between activity and semiconducting properties of pyrite electrodes", *J. Electroanal. Chem. Interfacial Electrochem.*, **70**: 265-275.

Buckley, A.N., Hamilton, I.C., and Woods, R., 1985, "Investigation of the surface oxidation of sulphide minerals by linear potential sweep voltammetry and X-ray photoelectron spectroscopy", in *Flotation of Sulphide Minerals*, (ed. K.S.E. Forssberg), Elsevier Science Publishers, B.V.

Hamilton, I.C. and Woods, R., 1981, "An investigation of surface oxidation of pyrite and pyrrhotite by linear potential sweep voltammetry", *J. Electroanal. Chem. Electrochem.*, **118**:327-343.

Trahar, W.J., 1984, "The influence of pulp potential in sulfide flotation", in *Principles of Mineral Flotation*, (eds. M.H. Jones and J.T. Woodcock), The Australasian Institute of Mining and Minerals Processing, Victoria, Australia, 117-136.

Young, C.A., Woods, R., and Yoon, R.-H, 1988, "A voltammetric study of chalcocite oxidation to metastable copper sulfides", in *Proc. Electrochemistry in Mineral and Metal Processing II*, (eds. P.E. Richardson and R. Woods), The Electrochemical Soc. Inc, **88-21**:3-17.

Zhu, X., Li, J., Bodily, D.M., and Wadsworth , M.E., 1992, "Transpassive oxidation of pyrite", in *Proc. Electrochemistry in Mineral and Metal Processing III*, (eds. R. Woods and P.E. Richardson), The Electrochemical Society Inc., **92-17**, 391-409.

Zhu, X., Wadsworth, M.E., Bodily, D.M. and Riley, A.M., 1991, "Surface properties of mineral and coal pyrite after electrochemical alteration", in *Processing and Utilization of high-sulfur Coals IV*, (eds. P.R. Dugan, D.R. Quigley and Y.A. Attia), 205.

END

DATE
FILMED
5/7/93